

ARTICLE

Open Access

# Oxidative stress activates NORAD expression by H3K27ac and promotes oxaliplatin resistance in gastric cancer by enhancing autophagy flux via targeting the miR-433-3p

Jizhao Wang<sup>1</sup>, Yuchen Sun<sup>2</sup>, Xing Zhang<sup>3</sup>, Hui Cai<sup>4</sup>, Cheng Zhang<sup>1</sup>, Hangying Qu<sup>1</sup>, Lin Liu<sup>1</sup>, Mingxin Zhang<sup>5</sup>, Junke Fu<sup>1</sup>, Jia Zhang<sup>1</sup>, Jiansheng Wang<sup>1</sup> and Guangjian Zhang<sup>1</sup>

## Abstract

Oxaliplatin resistance undermines its curative effects on cancer and usually leads to local recurrence. The oxidative stress induced DNA damage repair response is an important mechanism for inducing oxaliplatin resistance by activating autophagy. ELISA is used to detect target genes expression. TMT-based quantitative proteomic analysis was used to investigate the potential mechanisms involved in NORAD interactions based on GO analysis. Transwell assays and apoptosis flow cytometry were used for biological function analysis. CCK-8 was used to calculate IC50 and resistance index (RI) values. Dual-luciferase reporter gene assay, RIP and CHIP assays, and RNA pull-down were used to detect the interaction. Autophagy flux was evaluated using electron microscope and western blotting. Oxidative stress was enhanced by oxaliplatin; and oxaliplatin resistance gastric cancer cell showed lower oxidative stress. TMT labeling showed that NORAD may regulate autophagy flux. NORAD was highly expressed in oxaliplatin-resistant tissues. In vitro experiments indicate that NORAD knockdown decreases the RI (Resistance Index). Oxaliplatin induces oxidative stress and upregulates the expression of NORAD. SGC-7901 shows enhanced oxidative stress than oxaliplatin-resistant cells (SGC-7901-R). NORAD, activated by H3K27ac and CREBBP, enhanced the autophagy flux in SGC-7901-R to suppress the oxidative stress. NORAD binds to miR-433-3p and thereby stabilize the ATG5- ATG12 complex. Our findings illustrate that NORAD, activated by the oxidative stress, can positively regulate ATG5 and ATG12 and enhance the autophagy flux by sponging miR-433-3p. NORAD may be a potential biomarker for predicting oxaliplatin resistance and mediating oxidative stress, and provides therapeutic targets for reversing oxaliplatin resistance.

## Background

Gastric cancer is among the most lethal cancers worldwide, and has a median recurrence time of

11.7 months<sup>1</sup>. The poor prognosis is due to the tendency to recurrence and the poor therapeutic effects of chemotherapy<sup>2</sup>. Platinum-based chemotherapy, such as that with XELOX (oxaliplatin and capecitabine), can significantly improve the survival rate and control local recurrence<sup>3</sup>. Additionally, oxaliplatin-containing regimens may be superior to other platinum-containing regimens<sup>4</sup>. For example, oxaliplatin can prolong less-than-a-month overall survival compared with cisplatin<sup>5</sup>. In clinical practice, resistance to oxaliplatin usually leads to the failure of chemotherapy<sup>6</sup>. Therefore, in this

Correspondence: Jia Zhang (zhangjiaxjtu@xjtu.edu.cn) or Jiansheng Wang (wangjsh@xjtu.edu.cn) or Guangjian Zhang (michael8039@163.com)

<sup>1</sup>Department of Thoracic Surgery, The First Affiliated Hospital of Xi'an Jiaotong University, Xi'an, Shaanxi, China

<sup>2</sup>Department of Radiation Oncology, The First Affiliated Hospital of Xi'an Jiaotong University, Xi'an, Shaanxi, China

Full list of author information is available at the end of the article

These authors contributed equally: Jizhao Wang, Yuchen Sun

Edited by G. M. Fimia

© The Author(s) 2021



**Open Access** This article is licensed under a Creative Commons Attribution 4.0 International License, which permits use, sharing, adaptation, distribution and reproduction in any medium or format, as long as you give appropriate credit to the original author(s) and the source, provide a link to the Creative Commons license, and indicate if changes were made. The images or other third party material in this article are included in the article's Creative Commons license, unless indicated otherwise in a credit line to the material. If material is not included in the article's Creative Commons license and your intended use is not permitted by statutory regulation or exceeds the permitted use, you will need to obtain permission directly from the copyright holder. To view a copy of this license, visit <http://creativecommons.org/licenses/by/4.0/>.

study, we aimed to investigate the key regulatory genes involved in modulating oxaliplatin resistance.

Oxaliplatin exerts its anticancer effects mainly through binding to and damaging DNA, thereby inhibiting DNA replication<sup>7</sup>. Oxaliplatin-induced DNA damage repair occurs primarily through the nucleotide excision repair (NER) pathway, the activation of which normally leads to oxaliplatin resistance<sup>8</sup>. In addition to NER, autophagy is also reported to be involved in regulating oxaliplatin resistance. For example, Ren et al. showed that autophagy activation induces oxaliplatin resistance in hepatocellular carcinoma, which can be reversed by miR-125b<sup>9</sup>. Moreover, autophagy activated by HMGB1 was also shown to play an important role in decreasing oxaliplatin sensitivity in colorectal cancer<sup>10</sup>. The ATG5-ATG12-ATG16 complex, which possesses E3 ubiquitin-like activity, is crucial for autophagosome formation. ATG16 mediates the localization of the complex to the phagophore assembly site and the ATG5-ATG12 conjugate catalyzes the covalent attachment of LC3 to PE<sup>11</sup>. Additionally, ATG7, an E1 ubiquitin-like enzyme, and ATG10, an E2 ubiquitin-like enzyme, are required for the initial conjugation of ATG5 and ATG12<sup>12</sup>. However, whether autophagy is involved in oxaliplatin resistance in gastric cancer is unknown. Several studies have indicated that autophagy can be induced by the oxaliplatin-related DNA damage response, which then promotes oxaliplatin resistance<sup>13,14</sup>.

Oxidative stress has been found to be associated to generate DNA damage and induce apoptosis<sup>15</sup>. To date, accumulating evidences have indicated the essential role of oxidative stress in mediating platinum resistance. Sen Wang et al. illustrated that PRDX2 induced by *H.pylori* infection suppressed oxidative stress and double-strand breaks to promote cisplatin resistance<sup>16</sup>. Besides, reactive oxygen species production can be increased by cannabidiol, resulting in enhanced autophagy and sensitizing colorectal cancer cells to oxaliplatin<sup>14</sup>. In this context, we assumed the essential role of oxidative stress in mediating oxaliplatin resistance by regulating DNA damage response and autophagy.

Increasing evidence has indicated that microRNAs (miRNAs) and long noncoding RNAs (lncRNAs) are important for mediating multidrug resistance<sup>17</sup>. NORAD was identified and named by Sungyul et al., who reported that NORAD (noncoding RNA activated by DNA damage) was induced by DNA damage and showed strong regulatory activity towards Pumilio-Fem3-binding factor (PUF), which regulates downstream target mRNAs by activating the deadenylation and decapping process<sup>18</sup>. Our group previously reported that NORAD can be induced by radiation, indicating its potential involvement in DNA damage responses<sup>19</sup>. Moreover, accumulating evidence has indicated that NORAD mostly resides in the cytoplasm, and that NORAD may act as a target miRNA

sponge and reverse their biological functions, including for miR-656-3p, miR-615-3p, and miR-202-5p<sup>19–21</sup>. Analysis using the UCSC genome browser led us to predict that H3K27ac may be enriched at the NORAD promoter and act as an important regulator of NORAD expression<sup>22</sup>. Histone H3 lysine 27 acetylation (H3K27ac) is usually found at transcription start sites, and interacts with active enhancers to promote gene expression<sup>23</sup>. CREB-binding protein (CBP) and P300, acting as the acetyltransferase, account for the H3K27ac in the promoter region of target genes to exert their transcriptional coactivator function<sup>24,25</sup>. A previous study reported that H3K27ac regulates the expression of *GLI1*, which is induced by cisplatin in a dose-dependent manner<sup>26</sup>. Therefore, we hypothesized that oxaliplatin-related DNA damage responses may upregulate the levels of H3K27ac, leading to the overexpression of NORAD and consequently oxaliplatin resistance.

In this study, using online bioinformatics tool, Starbase V2.0, we identified that miR-433-3p may be associated with oxaliplatin resistance<sup>27</sup>. MiR-433-3p is a potential tumor suppressor in esophageal cancer and glioma<sup>28,29</sup>. Importantly, miR-433-3p can enhance the sensitivity of glioma cells to temozolomide, which also induces DNA damage<sup>29</sup>. We also noticed that miR-433-3p is predicted to bind to the 3'-UTR of *ATG5* and *ATG12*<sup>27</sup>. This suggested that NORAD could compete with miR-433-3p for binding to *ATG5* and *ATG12*, thereby enhancing the autophagy flux and promoting oxaliplatin resistance.

## Methods

### Cell culture, transfection, and transduction

The SGC-7901 and KATO III cell lines were purchased and authenticated from the Cell Bank of the Chinese Academy of Sciences Typical Culture Preservation Committee (Shanghai, China); The GES-1 cell line was purchased from American Type Culture Collection (ATCC, Manassas, USA). SGC-7901, KATO III, and GES-1 were cultured in 1640-medium supplemented with 10% fetal bovine serum (FBS; ThermoFisher Scientific, Shanghai, China) at 37 °C and 5% CO<sub>2</sub>.

Lentiviral constructs for NORAD and miR-433-3p knockdown, miR-433-3p overexpression, and respective negative controls (NCs) were synthesized by Genechem (Shanghai, China). Lentiviral constructs were transduced into target cells at the concentration of  $1 \times 10^8$  TU/mL with transduction enhancement P solution. hU6-MCSU-biquitin-EGFP-IRES-puromycin was used as the vector for the miR-433-3p overexpression lentivirus; hU6-MCSCMV-EGFP was used as the vector for the NORAD and miR-433-3p knockdown lentiviruses. The NORAD knockdown plasmid, NORAD overexpression plasmid containing the wild-type binding site for miR-

433-3p, NORAD overexpression plasmid containing a mutated binding site for miR-433-3p, miR-433-3p overexpression plasmid, and miR-433-3p knockdown plasmid were designed and synthesized by Genechem. The plasmid vector used was CMV-MCS-SV4-Neomycin. Cells were transfected with the above plasmids using Lipofectamine 3000 (Thermo Fisher Scientific, Shanghai, China) for analysis of autophagy and apoptosis.

### Patients

Our group has recruited 379 T1b-T3 stage gastric cancer patients, who were pathologically diagnosed from 2013 January to 2015 December in First affiliated hospital of Xi'an Jiaotong University and First affiliated hospital of Xi'an medical hospital. Our study has been approved by ethnics committee of First affiliated hospital of Xi'an Jiaotong University and ethnics committee of First affiliated hospital of Xi'an medical hospital. Our study has been carried out according to the declaration of Helsinki. Ever patient recruited was informed and signed the consent for acquiring their tissues.

### Whole-genome and miRNA sequencing chips

Twenty GeneChip PrimeView Human gene expression arrays (100-format, Affymetrix) were used for 10 gastric cancer tissues and corresponding adjacent normal tissues. The Agilent RNA 6000 Nano Kit was used for RNA quality control and the GeneChip 3' IVT PLUS Kit was used for in vitro transcription. The GeneChip Hybridization Wash and Stain Kit was used for chip hybridization, washing, and staining. Finally, chips were scanned by GeneChip Scanner 3000. The above process was assisted, advised, and supervised by Genechem. For miRNAs, 20 GeneChip miRNA 4.0 chips (100-format, Affymetrix) were used. The Agilent RNA 6000 Nano Kit was used for RNA quality control. The FlashTag Biotin HSR RNA Labeling Kit was used for miRNA labeling. Chip hybridization, washing, staining, and scanning was as for the whole-genome chip process. The above process was assisted, advised, and supervised by Genechem. TCGA and GTEx gastric cancer patient data were also included to confirm the result of our whole-genome sequencing data analysis.

### Quantitative analysis of TMT (Tandem Mass Tag)-labeled proteins

SGC-7901 cells were used as controls, and NORAD knockdown SGC-7901 cells as the experimental group. SDT lysis buffer was used for protein extraction. Extracted protein (20  $\mu$ g) was electrophoresed on 12% SDS-PAGE at 220 V for 40 min. FASP enzymolysis was then carried out with trypsin buffer; a C18 Cartridge was used for desalination of peptide fragments. The Easy nLC system was used for chromatography. The whole

process was assisted, advised, and supervised by Genechem.

### RNA extraction and qRT-PCR

TRIzol reagent (Invitrogen, Carlsbad, CA, USA) was used for total RNA extraction. The PrimeScript™ RT reagent Kit (TaKaRa, Dalian, China) was used for reverse transcription. SYBR Premix Ex Taq™ II (TaKaRa) was used for qPCR. The NucleoSpin miRNA kit (TaKaRa) was used for purification of the RNA used for miRNA qRT-PCR. The purified RNA was then treated with DNase I if the RNA was extracted from transfected cells. The Mir-X miRNA qRT-PCR TB Green Kit (TaKaRa) was used for reverse transcription and qPCR. *GAPDH* was used as the control for NORAD, and *U6* for miR-433-3p. The following primers were used: *GAPDH*, forward: 5'-TGCCAAATATGACATCAAGAA-3' and reverse: 5'-GGAGTGGTGTCGTCGCTGTTG-3'; *NORAD*, forward: 5'-AAGCTGCTCTCAACTCCACC-3' and reverse: 5'-GGACGTATCGCTTCCAGAGG-3'; and miR-433-3p, forward: 5'-CGATCATGATGGGCTCCTCG-3' and reverse: 5'-GTGCAGGGTCCGAGGT-3'.

### Protein extraction and western blot

Total protein was extracted using RIPA buffer (Sigma-Aldrich, Cambridge, MA, USA), which was then validated by BCA (Sigma-Aldrich, Cambridge, MA, USA). Proteins were electrophoresed on 10% SDS-PAGE gels and then transferred onto PVDF membranes. The membranes were blocked with 5% nonfat milk in TBS-T for 2 h at room temperature. Primary antibodies were incubated overnight at 4 °C. The following day, secondary antibodies were incubated for 1 h at room temperature.

### Analysis of autophagy

SensGFP-StubRFP-LC3 lentivirus, which was constructed by Genechem, were used to transfect target cells. After 24 h of transfection, puromycin was used to eliminate unaffected cells for 3 days. Then cells were resuspended and plated into 96-well plates at the concentration of  $1 \times 10^4$ /well for 18 h. Confocal Quantitative Image cytometer (YOKOGAWA, Tokyo, Japan) was used to scan and analyze the cells.

### Construction of the oxaliplatin-resistant cell line

The oxaliplatin-resistant SGC-7901 and KATO III cell line were named SGC-7901-R and KATO III-R respectively. First, SGC-7901 and KATO III cells were incubated with 2  $\mu$ g/mL oxaliplatin for 24 h; then, the medium was changed to oxaliplatin-free medium and cell growth was observed. The above process was repeated several times until SGC-7901 and KATO III cells overcame inhibition of proliferation. The oxaliplatin concentration was then increased to 3, 4, 6, 8, and 10  $\mu$ g/mL. Finally, SGC-7901

and KATO III cells that survived with 10  $\mu\text{g}/\text{mL}$  oxaliplatin were regarded as oxaliplatin-resistant (KATO III-R and SGC-7901-R).

#### IC50 and resistance index (RI)

Cell counting kit-8 (CCK-8, Apexbio, USA) was used to evaluate the viability of target cells. Cells ( $1 \times 10^5$ ) were added to each well and culture medium containing 1, 2, 4, 8, 16, 32, and 64  $\mu\text{g}/\text{mL}$  oxaliplatin was added to individual wells. After culturing for 48 h, 10  $\mu\text{L}$  of the CCK-8 solution was added to each well and incubated for 2 h. The absorbance at 490 nm was measured for each well. The IC50 was calculated using GraphPad Prism 8.2 (GraphPad Software, La Jolla, CA, USA). The RI was calculated as IC50 of Resistant cells/IC50 of Parental cells.

#### Evaluation of oxidative stress

Superoxide Dismutase (SOD) assay kit, Malondialdehyde (MDA) assay kit and Glutathione Peroxidase (GSH-PX) assay kit were used to detect the level of SOD, MDA, and GSH in target cells and tissues according to manufactures' guides.

#### ROS production

DHE (Dihydroethidium) Assay Kit—Reactive Oxygen Species (ab236206, Abcam China, Shanghai, China) was purchased to measure the ROS level in live target cells. Total DHE fluorescence intensity represents the ROS generation. Around  $1 \times 10^5$  cells were resuspended and added to V-bottom plate, which was centrifuged at  $400 \times g$ . Then 130  $\mu\text{L}$  ROS staining buffer and 100  $\mu\text{L}$  Cell-Based Assay Buffer. The fluorescence intensity was measured using 480 nm excitation wavelength and 570 nm emission wavelength.

#### ChIP assay

The EZ-Magna ChIP™ A/G Chromatin Immunoprecipitation Kit (Sigma–Aldrich, Darmstadt, Germany) was used for the assay. Target cells were treated with formaldehyde to ensure the co-precipitation of DNA with proteins. The cells were then sonicated to generate 200–500 bp DNA fragments, which were validated by electrophoresis. Subsequently, the generated DNA fragments were immunoprecipitated with anti-H3K27ac and anti-CBP antibodies. An IgG antibody was used as the control. qPCR was used to detect NORAD expression.

#### RIP assay

Magna RIP™ RNA-Binding Protein Immunoprecipitation Kit (Millipore, Billerica, MA, USA) was used for RIP assay. RIP lysis buffer was used for lysing target cells and then Ago2 antibody was used for immunoprecipitation;

IgG antibody was used for control. The whole process was assisted, advised and supervised by Genecreate(Wuhan, China).

#### FISH

Cell slides were pretreated with HCL for 20 min, the 1% NaSCN at 80 °C for 30 min, and 4% pepsin at 37 °C for 10 min. The cells were then fixed in neutral formalin at room temperature for 10 min. Then, the cells were treated with a prehybridization solution (50% deionized formamide,  $5 \times \text{SSC}$ ,  $5 \times \text{Denhardt}$ , 0.02% SDS, 0.1 mg/mL yeast tRNA, 100  $\mu\text{g}/\text{mL}$  denatured and sheared salmon sperm DNA) at 50 °C for 2 h. The cells were then hybridized with a NORAD probe at 48 °C for 6 h. The cells were subsequently washed with  $2 \times \text{SSC}$  and 0.3% NP-40 at 72 °C for 30 min and stained with DAPI for 5 min. The cells were observed under a confocal microscope.

#### Dual-luciferase reporter assay

NORAD overexpression plasmids containing either the wild-type NORAD binding site (NORAD-WT) or a mutated NORAD binding site (NORAD-Mut) for miR-433-3p and miR-433-3p overexpression plasmids were constructed by Genechem using GV272. The negative control vector was SV40-firefly\_Luciferase-MCS. Cells were co-transfected with NORAD and miR-433-3p overexpression plasmids, as follows: NORAD-WT + miR-433-3p, NORAD-Mut + miR-433-3p, NORAD-WT + NC, and NORAD-Mut + NC. After 48 h, firefly and *Renilla* luciferase activities were measured.

#### RNA pull-down assay

The biotinylated probes miR-433-3p-Wt and miR-433-3p-Mut were synthesized by Genecreate (Wuhan, China). The probe sequence for miR-433-3p-WT was AUCAUG AUGGGCUCCUCGGUGU and for miR-433-3p-Mut the sequence was AAGUACUAGGGCUCCUCGGUGU. Target cells were transfected with the above probes. After 48 h, the biotinylated RNA was bound to M-280 Streptavidin-coated MagneSphere particles using RNase-free bovine serum albumin (BSA) and yeast tRNA. After elution, RNA was combined, harvested, and purified. The RNA was then reverse-transcribed into cDNA and qPCR was used to evaluate NORAD enrichment.

#### Apoptosis

NORAD knockdown plasmids were used for transfection. The FITC Annexin V Apoptosis Detection Kit I (BD Pharmingen TM, New Jersey, USA) was used for apoptosis testing. Target cells were stained with Annexin V–FITC at room temperature for 15 min, followed by flow cytometry to detect fluorescence intensity.

### Transwell assay

Cells ( $5 \times 10^5$ ) were plated into the upper chamber of Transwell plates for migration tests; chambers with Matrigel-coated membranes were used for invasion tests. Culture medium supplemented with 20% FBS was added to the lower chambers. Cells were then cultured in serum-free medium in the upper chamber for 24 h at 37 °C and 5% CO<sub>2</sub>. Cells from the upper chambers were gently wiped off and those from the lower chambers were stained with crystal violet and counted under an optical microscope.

### Animal model

We have recruited 20 nude mice (20–25 g, 4 weeks old) in this study. The mice were purchased from Animal center of Xi'an Jiaotong University. The 20 nude mice were then grouped into four groups. No blinding was carried out when grouping the mice.  $1 \times 10^6$  SGC-7901, SGC-7901-R, and SGC-7901-R NORAD knockdown and relevant NC cells were injected into the right flank of mice to produce xenograft tumors. When the volume of xenograft tumors reached  $\sim 300\text{--}400\text{ mm}^3$ , we began treating mice with 10  $\mu\text{g}/\text{kg}$  oxaliplatin every week for 2 weeks through tail vein injection. After 4 weeks, xenograft tumors were harvested for further analysis.

### Statistics

Data analysis was performed using R 3.3.1. GraphPad Prism 8.2 was used for graphing. ImageJ was used to quantify the western blotting and PCR results. Data are presented as means  $\pm$  standard deviation. Paired *t*-tests were used for comparison between two groups. The R package WGCNA was used to perform WGCN analysis. The R package randomForest was used to construct the random-forest model.

## Results

### Oxidative stress plays an important part in mediating oxaliplatin resistance of gastric cancer cell

We generated oxaliplatin-resistant SGC-7901 and KATO III cell lines, which we named SGC-7901-R and KATO III-R. The IC<sub>50</sub> value for SGC-7901 cells was 2.97  $\mu\text{g}/\text{mL}$  (Fig. 1A), while for the SGC-7901-R cells, the IC<sub>50</sub> was 18.73  $\mu\text{g}/\text{mL}$  (Fig. 1B). This resulted in a RI (Resistance index) of 6.31 (18.73/2.97), indicating that SGC-7901-R cells were oxaliplatin resistant. Besides, after treated with 5 mM NAC, the IC<sub>50</sub> value for SGC-7901 and SGC-7901-R were 2.84 and 6.11  $\mu\text{g}/\text{mL}$  respectively; and the RI was 2.15 (6.11/2.84), which was significantly decreased compared with 6.31. The IC<sub>50</sub> value for KATO III and KATO III-R were 2.58 and 10.45  $\mu\text{g}/\text{mL}$  respectively, the RI was 4.05 (10.45/2.58); and 5 mM NAC significantly decreased the RI (5.60/2.30 = 2.43) as well (Fig. 1C, D).

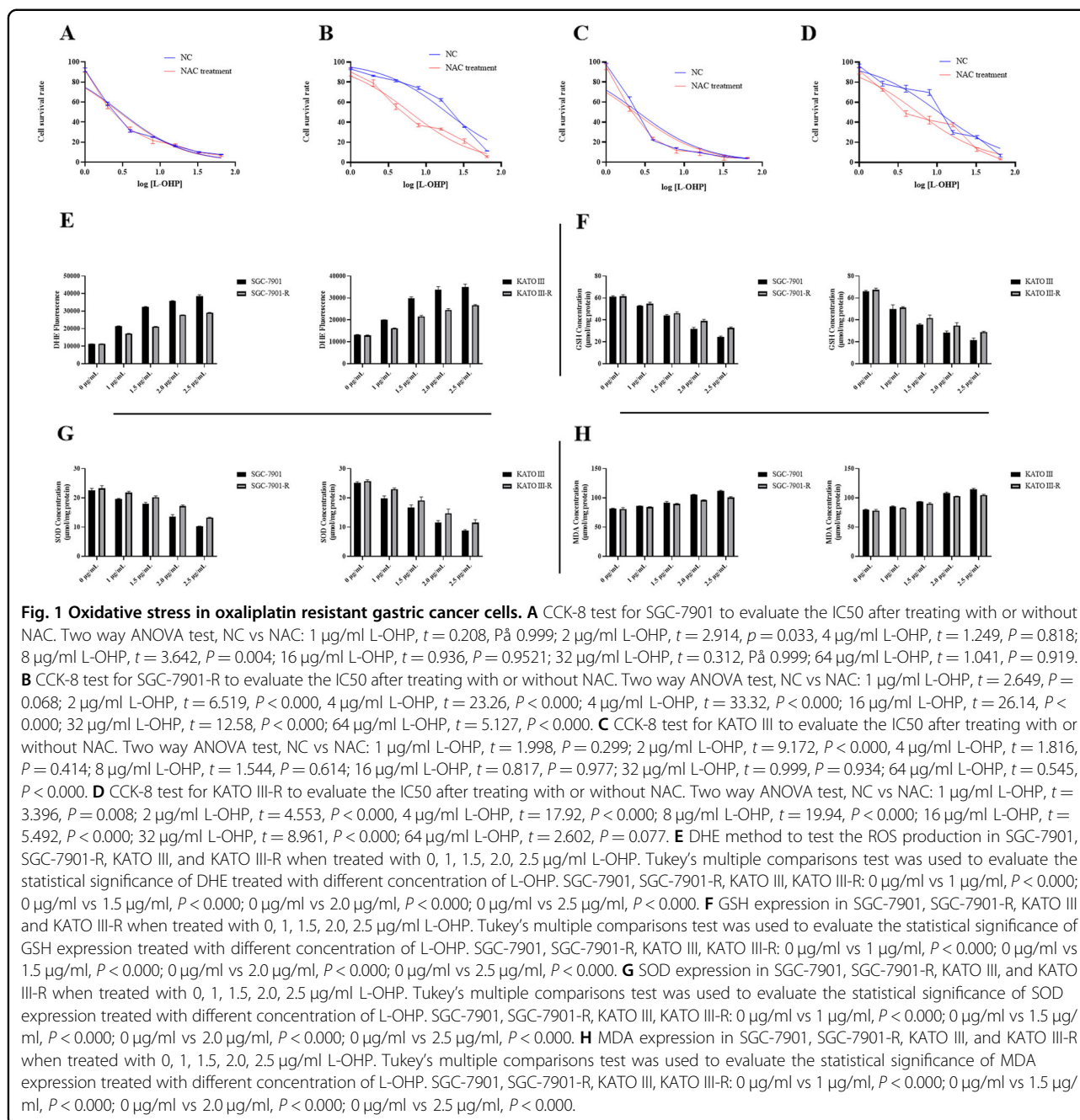
When treated with oxaliplatin, the ROS production in gastric cancer cells was significantly enhanced (Fig. 1E); besides GSH and SOD were decreased and MDA level was increased (Fig. 1F–H). Moreover, we noticed that ROS production and MDA were lower and GSH and SOD level were higher in oxaliplatin-resistant cells than that in their parental cells (Fig. 1E–H).

### NORAD was associated with DNA damage and autophagy in gastric cancer cell

We recruited 10 gastric cancer patients who had been subjected to XELOX treatment. To identify XELOX resistance-associated genes and miRNAs, we used weighted gene co-expression network analysis (WGCNA) to group them into several modules based on XELOX response evaluation and ypStage. For the whole-genome chip data, WGCNA showed that only the magenta module was associated with XELOX response and ypStage (Fig. 2A). For miRNA chip data, the blue module was associated with XELOX response and negatively related to ypStage; however, the result was not significant (Fig. 2B). We then selected the magenta module for further Random forest model analysis. The results showed that the five most important genes were: 11757398\_x\_at (NORAD), 11760870\_at, 11728805\_a\_at, 11728003\_a\_at and 11737881\_x\_at (Fig. 2C). Therefore, we further evaluated the role and mechanism involved in NORAD-mediated XELOX resistance. We used the online bioinformatics tool Starbase V3.0 to predict potential NORAD targets, and found that miR-433-3p was at the intersection of those targets with the blue module. TMT labeling was then used to compare the differential expression of related proteins in NORAD knockdown SGC-7901 cells and NC SGC-7901 cells. Following GO pathway analysis indicated that NORAD may have a role in autophagosome assembly, DNA repair, mitophagy, apoptotic process, double-strand break repair via homologous recombination, extracellular matrix organization, and et al. (Fig. 2D). Among the autophagy-related genes, we noticed that the expression of ATG5 and ATG12 were upregulated by NORAD based on the TMT-labeling method (Fig. 2E, F). Additionally, the TCGA and GTEx data also showed positive correlations between NORAD and ATG5 (Fig. 2G) and ATG12 (Fig. 2H).

In 379 gastric cancer patients, we found that NORAD expressed higher in gastric cancer patients compared with adjacent normal gastric tissues; and miR-433-3p expressed lower in gastric cancer tissues (Fig. 2I). Moreover, NORAD and miR-433-3p differentially expressed between recurrent and nonrecurrent gastric cancer patients (Fig. 2J). Furthermore, NORAD and miR-433-3p was correlated with overall survival and cancer-specific survival (Fig. 2K–N).

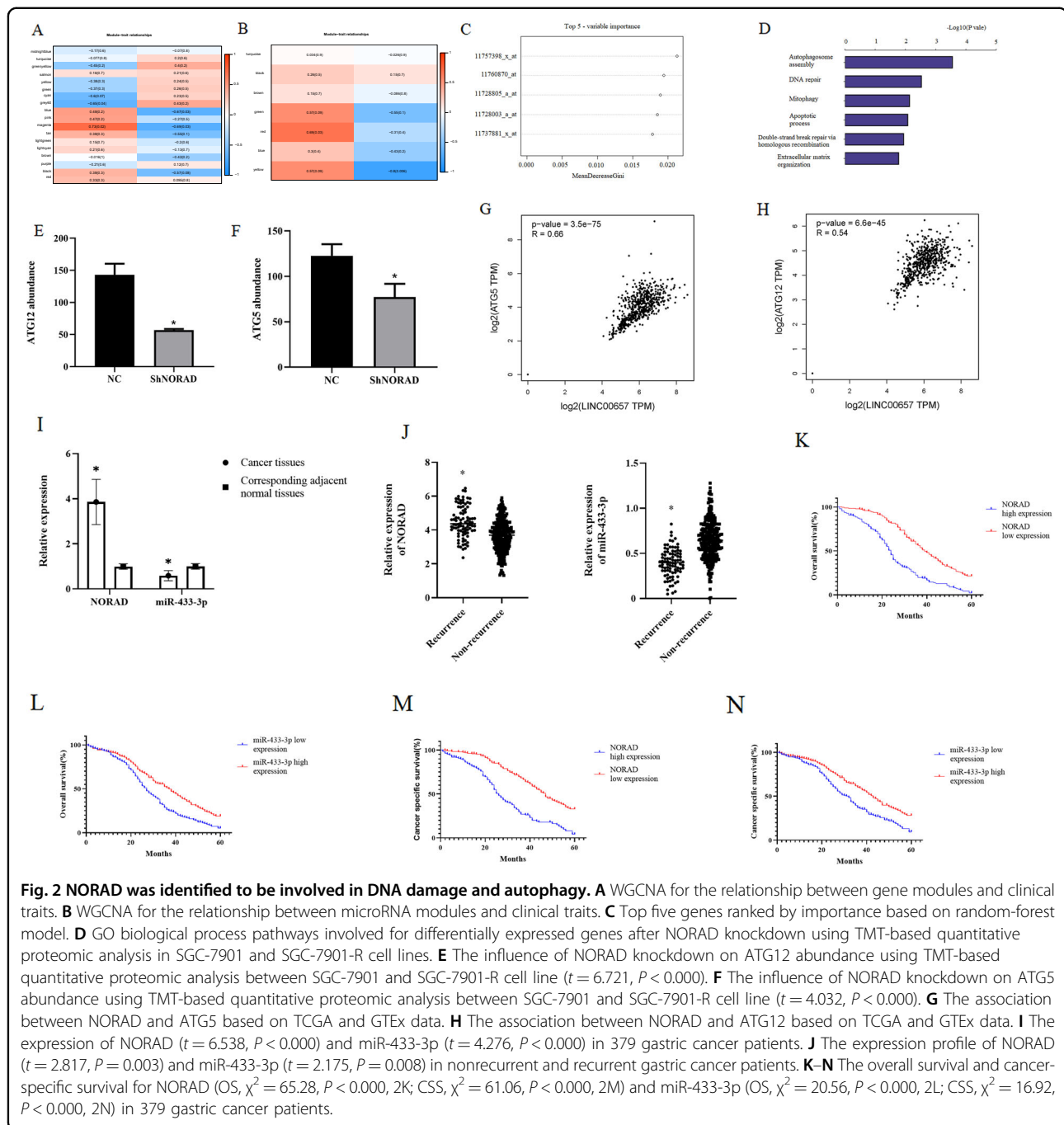




### NORAD was involved in regulating oxaliplatin resistance through mediating oxidative stress

We found that NORAD was highly expressed in gastric cancer cell lines compared to normal gastric epithelium cell line, GES-1 (Fig. 3A), and that NORAD expression was higher in oxaliplatin-resistant cells than their parental cells (Fig. 3B). After treated with 2 µg/mL oxaliplatin, the expression of NORAD is significantly enhanced in gastric cancer cells (Fig. 3C). We then stably knocked down NORAD expression in both oxaliplatin-resistant cells and parental cells (Fig. 3D). NORAD knockdown led to reduced

proliferation rates and IC<sub>50</sub> values in SGC-7901 (IC<sub>50</sub> = 2.24 µg/mL) and SGC-7901-R (IC<sub>50</sub> = 11.68 µg/mL) cell lines; and KATO III (IC<sub>50</sub> = 1.79 µg/mL) and KATO III-R (IC<sub>50</sub> = 4.76 µg/mL) cells (Fig. 3E), indicative of a potential relationship between NORAD and oxaliplatin resistance. We also found that apoptosis could be induced by NORAD knockdown in SGC-7901-R and KATO III-R (Fig. 3F), suggesting that NORAD could induce oxaliplatin resistance. Further transwell assay showed that the migration and invasion ability of SGC-7901-R and KATO III-R was significantly decreased (Fig. 3G).

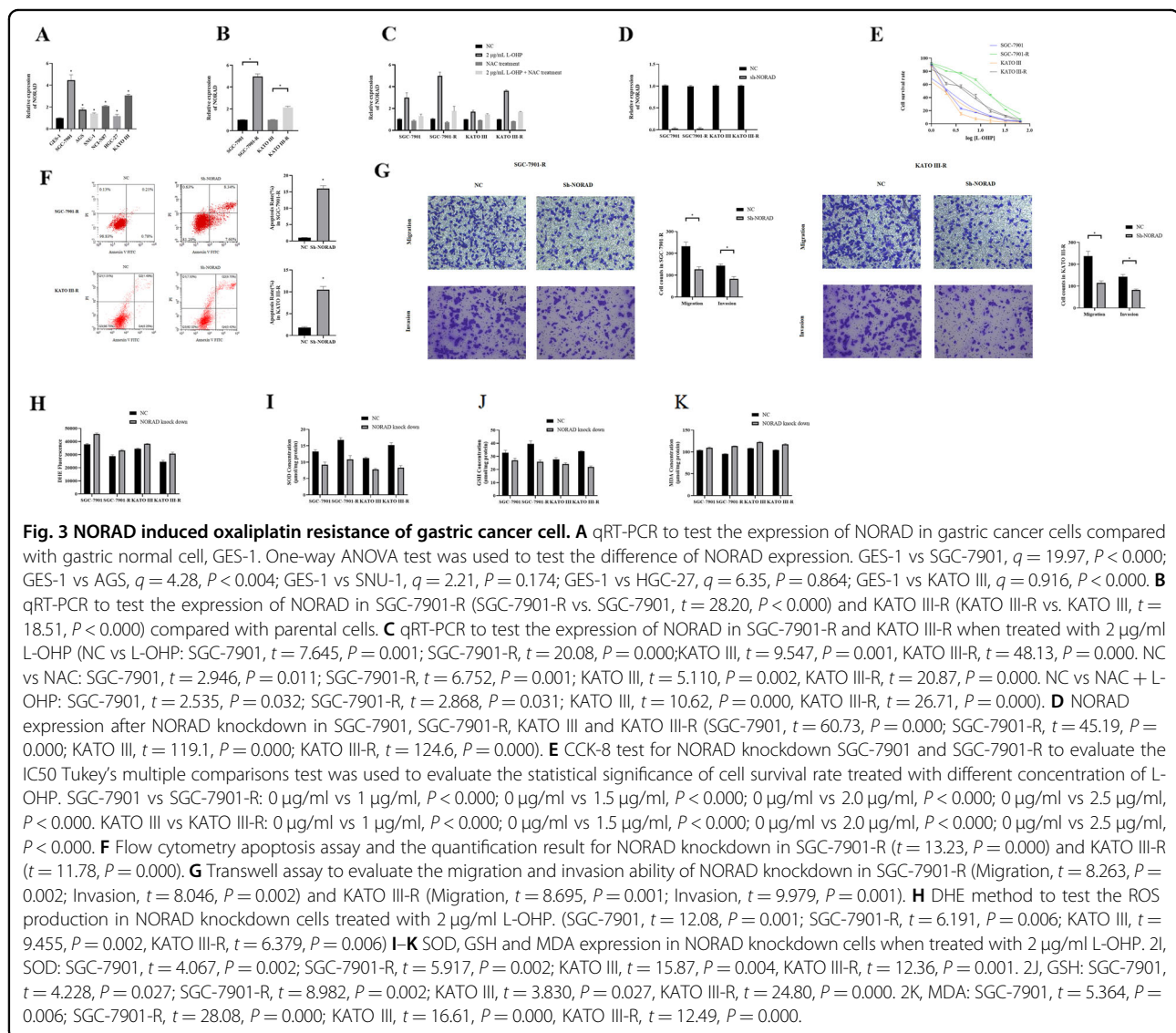


We then found that NORAD knockdown increased the ROS production and MDA level and decreased the SOD and GSH level in oxaliplatin-resistant cells and parental cells when treated with 2  $\mu\text{g}/\text{mL}$  oxaliplatin (Fig. 3H–K).

#### NORAD expression was induced by DNA damage repair response

Western blot analysis indicated that DNA-PKcs, ATR, Phospho-ATR, ATM, Phospho-ATM,  $\gamma\text{H2AX}$ , and H2AX were upregulated in oxaliplatin-resistant gastric cancer

cells, indicating that DNA damage repair response was activated in SGC-7901-R and KATO III-R cells (Fig. 4A, B). Analysis using the UCSC genome browser indicated that H3K27ac enrichment might occur at the NORAD promoter, regulating its expression (Fig. 4C). The FISH results showed that NORAD was distributed in the nucleus and plasma in both oxaliplatin-resistant cells and their parental cells (Fig. 4D). After oxaliplatin treatment, the H3K27ac levels were induced in SGC-7901-R and KATO III-R cells, whereas in SGC-7901 and KATO III



cells the levels of H3K27ac did not significantly increase (Fig. 4E). The FISH results showed that H3K27ac was predominantly distributed in the nucleus in oxaliplatin-resistant cells (Fig. 4F). Moreover, CREBBP (CREB-binding protein) expression was higher in oxaliplatin-resistant cells than that in parental cells (Fig. 4G). The FISH results demonstrated that CREBBP was mainly distributed in the nucleus in both oxaliplatin-resistant cells and parental cells (Fig. 4H).

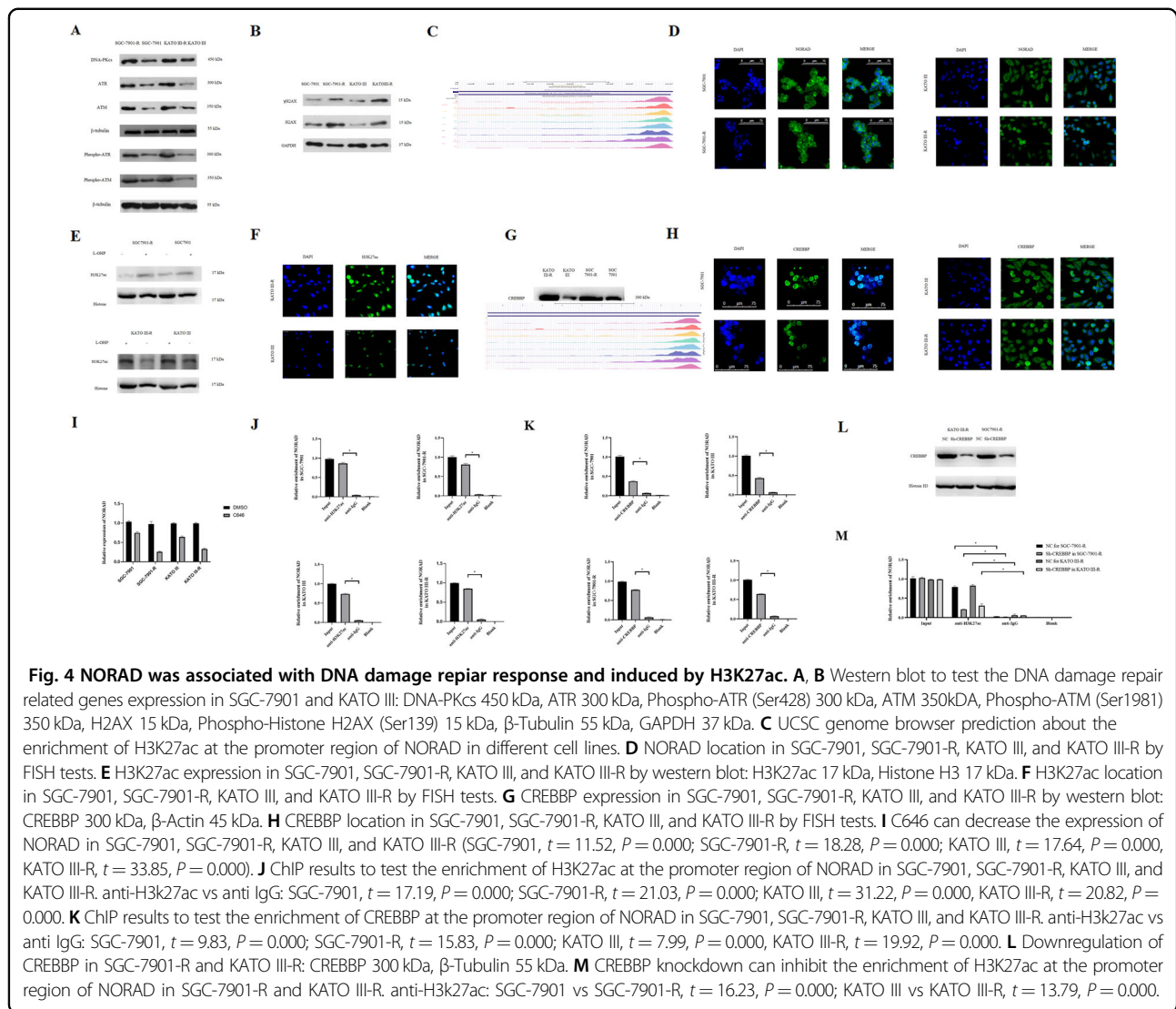
However, when we treated the cells with C646, a CREBBP inhibitor, we found that NORAD expression was significantly decreased in both cell lines when compared with DMSO-treated controls (Fig. 4I). These results indicated that CREBBP-mediated regulation of H3K27ac may be important for the induction of NORAD expression. The ChIP assay showed that H3K27ac and CREBBP were enriched at the NORAD

promoter of both gastric cancer cells and oxaliplatin-resistant cells (Fig. 4J, K). Furthermore, knockdown of CREBBP (Fig. 4L) reduced H3K27ac levels at the NORAD promoter in SGC-7901-R and KATO III-R cells (Fig. 4M). Combined, these results showed that the oxaliplatin-related DNA damage response can induce the binding of Histone H3 to CREBBP, thereby inducing NORAD expression.

#### Autophagy was associated with oxidative stress and oxaliplatin resistance

We found an enhanced autophagy flux in SGC-7901-R and KATO III-R cells (Fig. 5A). Further electron microscope was used to detect autophagosomes in oxaliplatin-resistant cells and their parental cells (Fig. 5B). In oxaliplatin-resistant cells, LC3B-II is highly expressed and p62 is lowly expressed compared with their parental





cells (Fig. 5C). Furthermore, we found that ATG5, ATG12, ATG7, and ATG10 expression was increased in oxaliplatin-resistant cells compared with that in parental cells (Fig. 5D), indicating enhanced phagophore to autophagosome transformation.

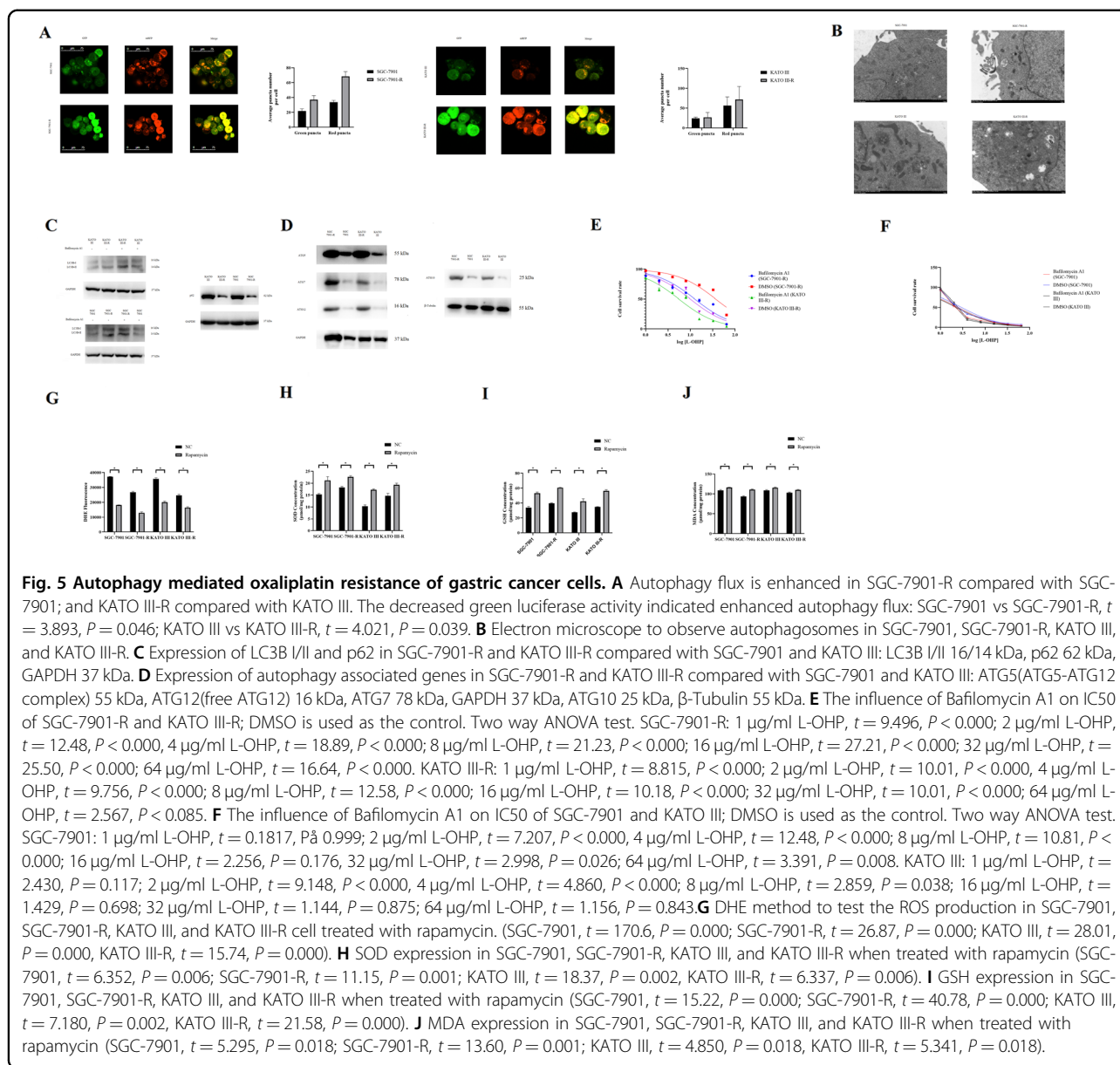
We also found that Bafilomycin A1 (10 nM for 18 h) could significantly decrease the IC<sub>50</sub> of SGC-7901-R (IC<sub>50</sub> = 12.55  $\mu$ g/ml) and KATO III-R (IC<sub>50</sub> = 5.52  $\mu$ g/ml) cells compared with DMSO (SGC-7901-R, IC<sub>50</sub> = 36.78  $\mu$ g/ml; KATO III-R, IC<sub>50</sub> = 9.95  $\mu$ g/ml) (Fig. 5E), while only slightly influencing that of SGC-7901 (IC<sub>50</sub> = 2.43  $\mu$ g/ml) and KATO III cells (IC<sub>50</sub> = 2.25  $\mu$ g/ml) (Fig. 5F), thereby decreasing the RI (5.16) compared with DMSO group (RI = 12.35) and KATO III-R (RI = 2.16 vs DMSO group, RI = 4.41) as well.

Besides, we found that Rapamycin, an autophagy enhancer, reduced the ROS production and MDA level and increased the GSH and SOD level (Fig. 5G–J) when

treated with 2  $\mu$ g/ml oxaliplatin. We assumed that the activation of autophagy assists in DNA repair response and reducing DNA damage; thereby, reduced the oxidative stress and promoted oxaliplatin resistance.

#### NORAD interacted with miR-433-3p to promote autophagy

When we knocked down NORAD in SGC-7901-R and KATO III-R cells, we found that LC3B-I expression was increased, and LC3B-II expression was inhibited, indicating that the autophagy flux was inhibited (Fig. 6A). Moreover, autophagy flux inhibition was detected by knocking down NORAD (Fig. 6B). We then knocked down NORAD expression in SGC-7901-R, and observed that ATG5 and ATG12 expression was inhibited; however, the expression of ATG7 and ATG10 remained unchanged (Fig. 6C). Based on Starbase V3.0, we predicted that miR-433-3p might be a target of NORAD (Fig. 6D).



We found that miR-433-3p expressed lowly in gastric cancer cells (Fig. 6E) and its expression was decreased in SGC-7901-R and KATO III-R cell line (Fig. 6F). miR-433-3p expression was increased in NORAD knockdown gastric cancer cells (Fig. 6G).

In the dual-luciferase reporter assay, the relative luciferase activity was significantly decreased in the NORAD-WT group in both SGC-7901 and SGC-7901-R cells (Fig. 6H), indicating that NORAG directly interacts with miR-433-3p.

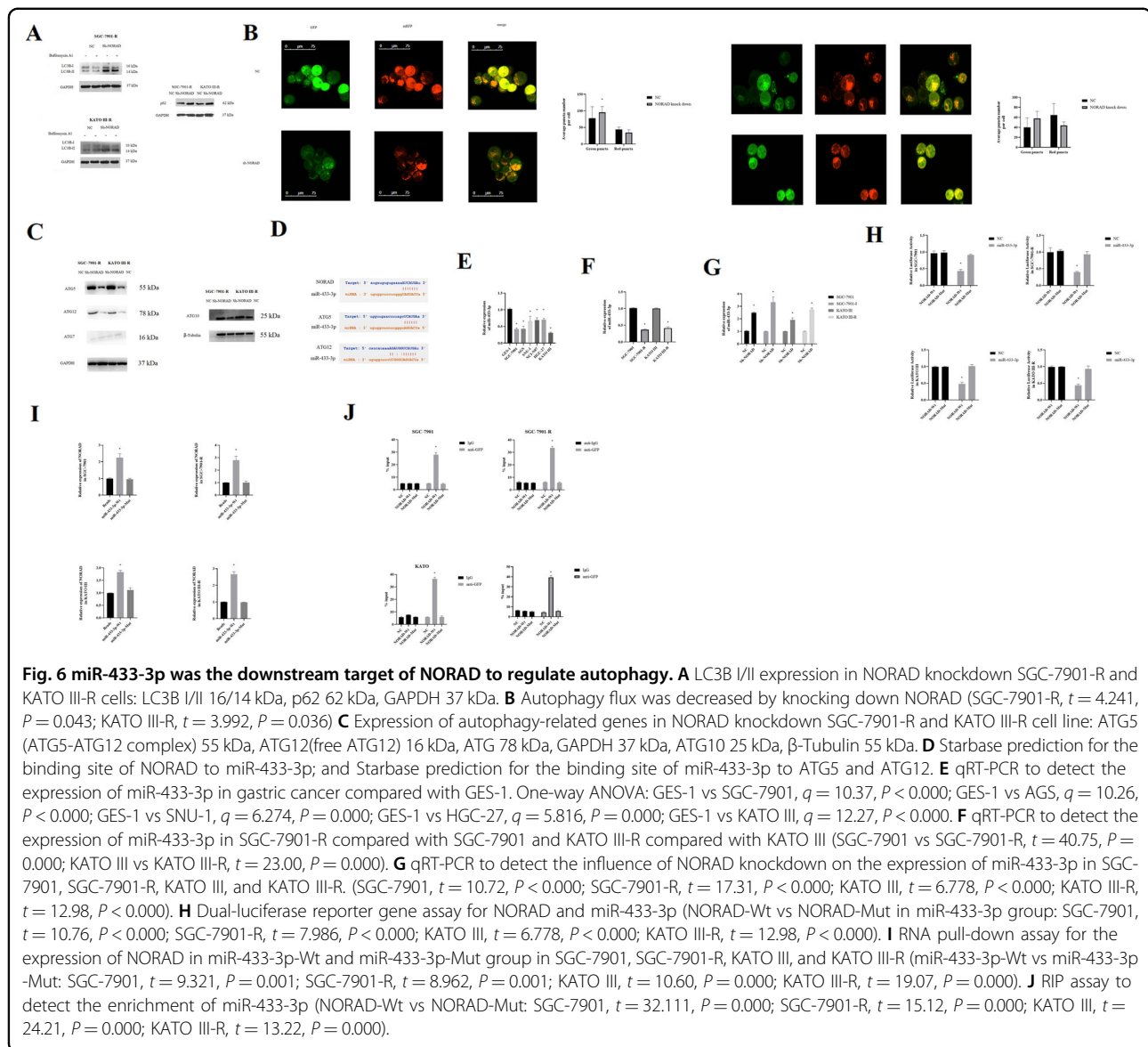
The RNA pull-down assay indicated that the expression of NORAD was higher in the miR-433-3p-Wt group compared with that in the miR-433-3p-Mut group in SGC-7901 and SGC-7901-R cells (Fig. 6I).

We then mutated NORAD for the RIP assay. The results showed that miR-433-3p was enriched in the NORAD-Wt group compared with that in the NORAD-Mut group (Fig. 6J).

Taken together, these results indicated that NORAD knockdown inhibited autophagy by decreasing the expression of miR-433-3p.

#### MiR-433-3p downregulated the expression of ATG5 and ATG12

When we overexpressed miR-433-3p in SGC-7901-R and KATO III-R, the expression of ATG5 and ATG12 was reduced (Fig. 7A). However, knockdown of miR-433-3p did not lead to a significant increase in the expression



of ATG5 or ATG12 in SGC-7901-R (Fig. 7B). The dual-luciferase reporter assay showed that miR-433-3p directly interacted with the 3'-UTR of *ATG12* (Fig. 7C), and the relative luciferase activity was also reduced in *ATG5* wild-type cells in SGC-7901-R and KATO III-R (Fig. 7D). Moreover, we found that overexpression of NORAD-WT induced the expression of ATG12 and ATG5 (Fig. 7E), whereas overexpression of NORAD-Mut did not (Fig. 7F). Furthermore, miR-433-3p knockdown could reverse the downregulation of ATG12 and ATG5 that was induced by NORAD knockdown (Fig. 7G).

#### NORAD knockdown mediated oxidative stress and inhibited oxaliplatin resistance in vivo

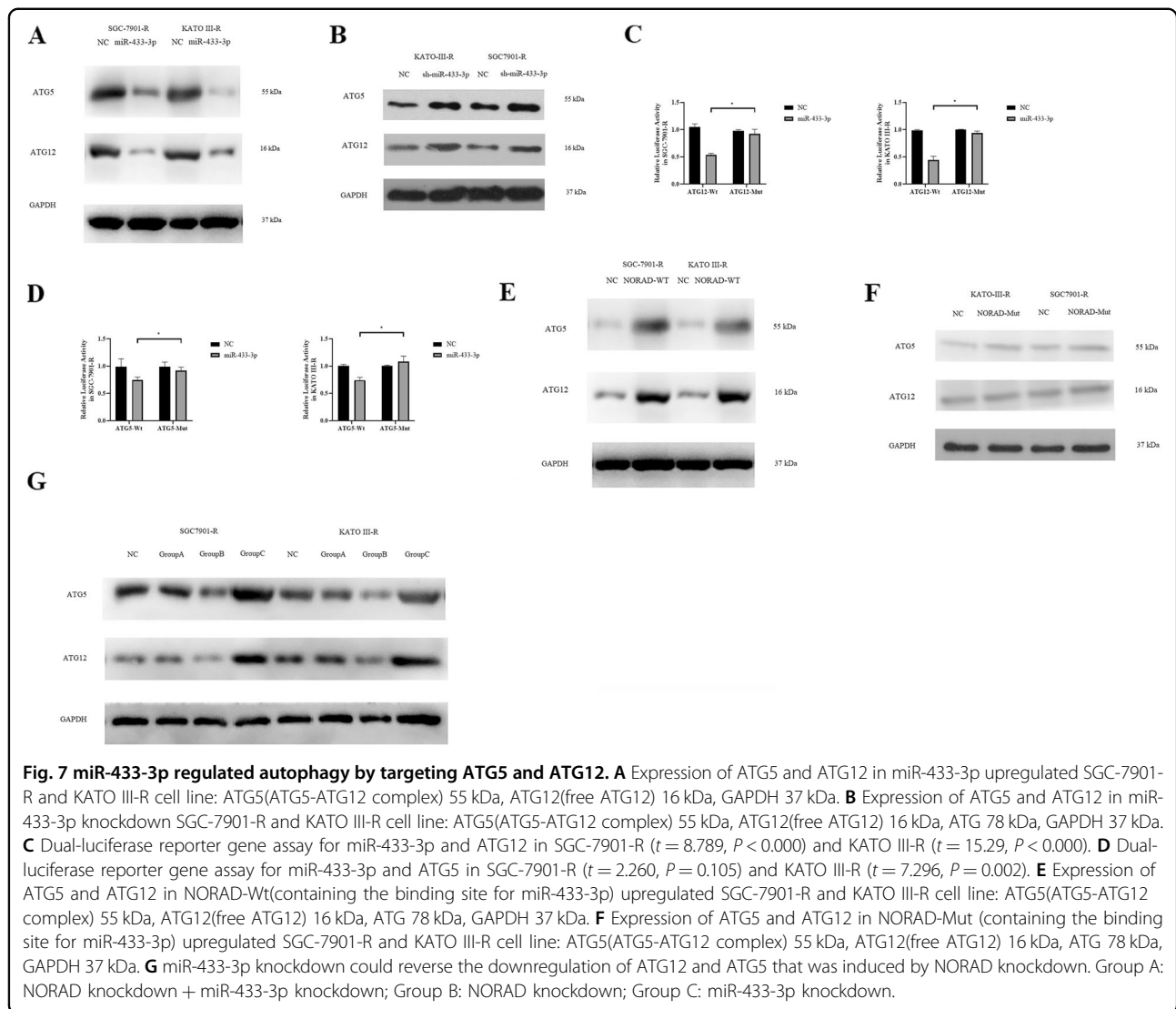
We have grafted SGC-7901 and SGC-7901-R cells into nude mice, who were subjected to 10  $\mu$ g/kg oxaliplatin

every week for 2 weeks. Then tumors were harvested (Fig. 8A) and the quantified estimated tumor burden results showed that SGC-7901-R mice can well tolerate oxaliplatin (Fig. 8B).

Then, mice, who were subjected to 10  $\mu$ g/kg oxaliplatin every week for 2 weeks, were grafted with NORAD knockdown and relevant NC SGC-7901-R cell line. Tumors were isolated after the same treatment stated above (Fig. 8C). The estimated tumor volume result indicated that NORAD knockdown can significantly inhibit the cell tolerance to oxaliplatin (Fig. 8D).

#### Discussion

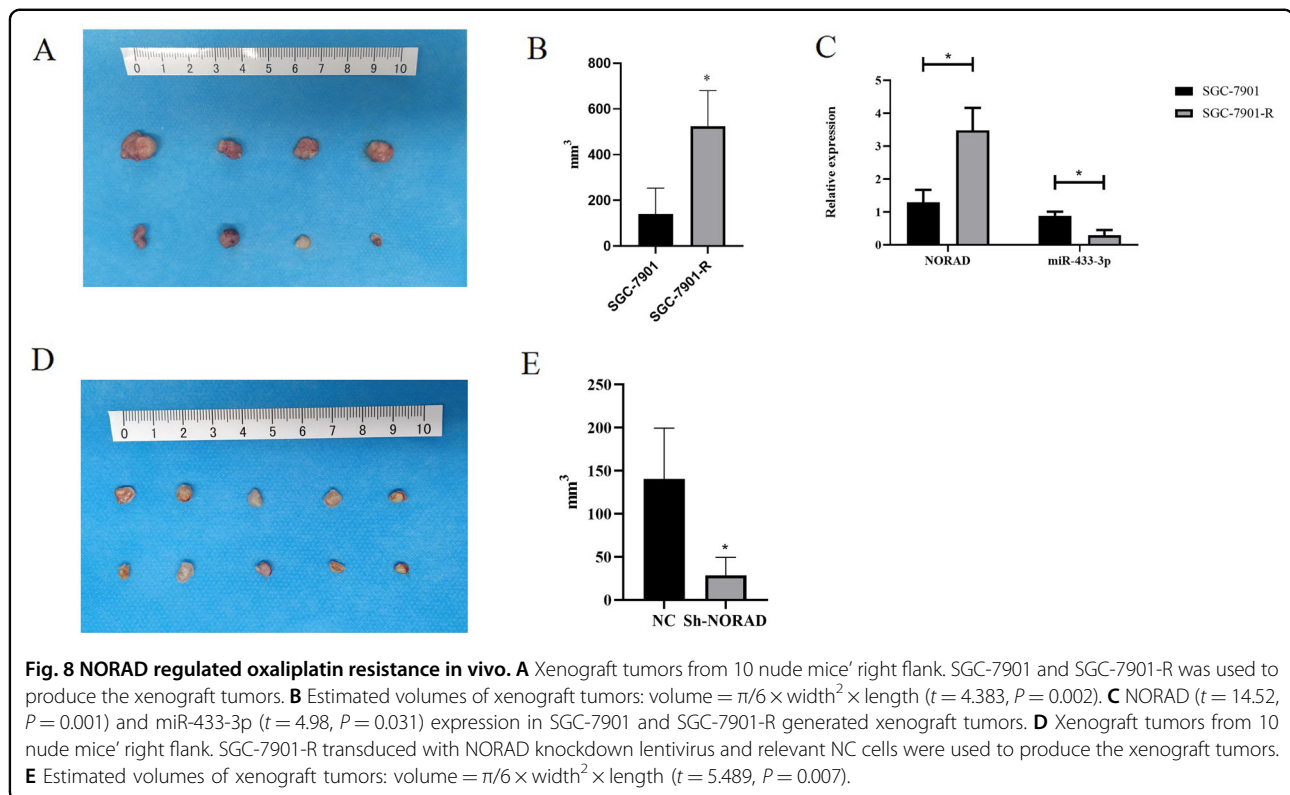
Oxaliplatin is a third-generation, platinum-containing anticancer agent, which exerts its anticancer effects through the induction of DNA damage and consequent



inhibition of DNA replication<sup>30</sup>. Oxaliplatin is well known for its greater efficacy in controlling cancer foci and inducing fewer side effects compared with other platinum-based drugs<sup>30</sup>. The employment of an oxaliplatin-based treatment strategy, such as post-operative XELOX therapy, has led to a significant improvement in the overall survival and reduction in the local recurrence rate of gastrointestinal cancers, especially gastric cancer<sup>31</sup>. However, some patients will experience oxaliplatin resistance and a dramatic reduction in the effectiveness of the drug, which may be due to continuous exposure to oxaliplatin<sup>32</sup>. Oxaliplatin resistance always leads to the failure of chemotherapy and results in recurrence and worse prognosis<sup>33</sup>. Therefore, it is vital that the molecular mechanisms involved in oxaliplatin resistance are clarified, thereby laying the foundation for the identification of novel therapeutic strategies.

In this manuscript, we found that oxidative stress, which can be induced by oxaliplatin treatment, is an important regulator in mediating oxaliplatin resistance. Furthermore, we noticed that SGC-7901-R has the ability to suppress oxidative stress. NORAD knockdown can abrogate the inhibiting ability of SGC-7901-R in ROS production. Therefore, we preliminary hypothesized that NORAD is overexpressed in response to ROS production and thus acted as an oxidative stress suppressor. Subsequently, we identified NORAD as a key regulator of oxaliplatin resistance. Our group previously reported the significant role of NORAD in mediating radiation resistance through the promotion of the DNA damage repair response<sup>19</sup>. In this manuscript, we have identified the enhanced DNA damage response in SGC-7901-R. We assumed that NORAD is induced by DNA damage and promotes DNA damage response; the continuous





activation of NORAD is essential for SGC-7901-R to suppress ROS production and resist oxidative stress.

Previously, a plethora of studies have presented that oxidative stress can induce the autophagy flux. We found that autophagy enhancer, rapamycin, can decrease the ROS production, indicating the important role of autophagy in regulating oxidative stress of SGC-7901-R cell.

Various studies have shown that activation of autophagy is associated with oxaliplatin resistance<sup>9,10,13,14</sup>. Here, we observed that autophagy flux was enhanced in oxaliplatin-resistant cells. The TMT-labeling result indicated that NORAD may promote autophagy by stabilizing the formation of the ATG5-ATG12 complex. NORAD knock-down inhibited the autophagy flux and significantly decreased the IC50 and RI of SGC-7901-R cells. This strongly suggested that autophagy is involved in oxaliplatin resistance in gastric cancer and inhibiting autophagy by targeting NORAD may be a potential strategy to reverse the oxaliplatin-resistant status of SGC-7901-R cells. Further experiments showed that NORAD did not affect the activity of ATG10 and ATG7, essential mediators of ATG5-ATG12 conjugation<sup>23</sup>. Bioinformatic analysis identified that miR-433-3p binds to the 3'-UTR of *ATG5* and *ATG12*, which was further confirmed by dual-luciferase reporter assays. Taken together, we have shown that NORAD sponges miR-433-3p, which upregulates the expression of *ATG5* and *ATG12*, thereby enhancing the autophagy flux.

As previously stated, oxaliplatin mainly causes DNA damage to exert its anticancer effects, indicating that activation of the DNA damage repair response is largely involved in mediating oxaliplatin resistance<sup>7</sup>. In this study, we observed that DNA damage repair was constitutively activated in oxaliplatin-resistant cells. Furthermore, we also found aberrantly high levels of H3K27ac, a form of histone acetylation mainly found in the promoter region of specific genes in oxaliplatin-resistant cells that promotes their expression<sup>34</sup>. As we found that H3K27ac is significantly enriched in the promoter region of NORAD, as assessed through UCSC prediction and ChIP results, we think that the oxaliplatin-mediated DNA damage repair response may induce the expression of NORAD to exert its regulatory function in oxaliplatin resistance by facilitating H3K27ac.

Accumulating evidence supports that diverse noncoding RNAs, including lncRNAs and miRNAs, have crucial biological functions in drug resistance<sup>35</sup>. For example, MALAT1 sponges miR-23b-3p to promote autophagy-related chemoresistance, giving rise to the vincristine resistance<sup>36</sup>. Moreover, the RNA gene *TINCR* can promote EMT through competing for the binding site of miR-125b on *HER2*, resulting in the trastuzumab resistance<sup>37</sup>. The FISH results indicated that NORAD is primarily localized in the cytoplasm, suggesting that NORAD may act as a sponge and compete with miRNAs for the binding to target gene promoters. Based on the



miRNA chip and bioinformatic analyses, we propose that NORAD may act as a molecular sponge for miR-433-3p.

## Conclusions

Graphical In conclusion, oxidative stress is enhanced by treating with oxaliplatin. NORAD knockdown induced oxidative stress by impairing SOD and GSH expression in SGC-7901-R. Then, oxaliplatin-induced DNA damage repair response can induce H3K27ac and activate CREBBP, which are enriched at the promoter region of NORAD, thereby upregulating its expression. NORAD will then enhance the autophagy flux by stabilizing ATG5-ATG12 conjugation through sponging miR-433-3p, leading to enhanced oxidative stress, and finally resulting in oxaliplatin resistance. Targeting NORAD can reverse the oxaliplatin-resistant status of SGC-7901-R cells, suggesting that targeting NORAD may be a novel therapeutic strategy for suppressing oxaliplatin resistance.

## Funding

This article is funded by National natural and science foundation, the grant number is 81702430; and Natural Science Foundation of Shaanxi Province, the grant number is 2019JM-599; Shaanxi key research and development plan, 2018SF-022; Foundation of First affiliated hospital of XJTU, XJTU1AF-CRF-2017-026; Wu jieping medical foundation, 320.2730.1877.

## Author details

<sup>1</sup>Department of Thoracic Surgery, The First Affiliated Hospital of Xi'an Jiaotong University, Xi'an, Shaanxi, China. <sup>2</sup>Department of Radiation Oncology, The First Affiliated Hospital of Xi'an Jiaotong University, Xi'an, Shaanxi, China. <sup>3</sup>Department of Hepatology Surgery, The First Affiliated Hospital of Xi'an Jiaotong University, Xi'an, Shaanxi, China. <sup>4</sup>Department of Vascular Surgery, The First Affiliated Hospital of Xi'an Jiaotong University, Xi'an, Shaanxi, China. <sup>5</sup>Department of Gastroenterology, The First Affiliated Hospital of Xi'an medical University, Xi'an, Shaanxi, China

## Author contributions

J.W. and Y.S. worked for the in vitro experiments and wrote the manuscript. X. Z., H.C., and C.Z. worked for the in vivo experiments and assisted in in vitro experiments. H.Q. and L.L. assisted in in vitro experiments and collected the gastric cancer tissues and carried out the follow-up. G.Z., M.Z., and J.F. guided and supervised the animal model of this study. G.Z. and J.Z. sponsored and supervised the in vitro and in vivo experiments. G.Z. and J.W. designed the study and carried out the quality control.

## Data availability

Data would be made available on request.

## Materials availability

Materials would be made available on request.

## Conflict of interest

The authors declare that they have no conflict of interest.

## Ethics approval and consent to participate

This study was approved by the Ethics Committee of First Affiliated Hospital of Xi'an Jiaotong University for carrying out experiments using patients' tissues and clinical data and animal model.

## Consent for publication

All co-authors have consented for publication.

## Publisher's note

Springer Nature remains neutral with regard to jurisdictional claims in published maps and institutional affiliations.

**Supplementary Information** accompanies this paper at (<https://doi.org/10.1038/s41419-020-03368-y>).

Received: 3 June 2020 Revised: 3 December 2020 Accepted: 4 December 2020

Published online: 18 January 2021

## References

- Datta, J. et al. Poor survival after resection of early gastric cancer: extremes of survivorship analysis reveal distinct genomic profile. *Br. J. Surg.* **107**, 14–19 (2020).
- Van Cutsem, E., Sagaert, X., Topal, B., Haustermans, K. & Prenen, H. Gastric cancer. *Lancet* **388**, 2654–2664 (2016).
- Reddavid, R. et al. Neoadjuvant chemotherapy for gastric cancer. Is it a must or a fake? *World J. Gastroenterol.* **24**, 274–289 (2018).
- Ilson, D. H. Advances in the treatment of gastric cancer. *Curr. Opin. Gastroenterol.* **33**, 473–476 (2017).
- Sasaki, K. et al. Validity of neoadjuvant chemotherapy with docetaxel, cisplatin, and S-1 for resectable locally advanced gastric cancer. *Med. Oncol.* **34**, 193 (2017).
- Cartwright, E. & Cunningham, D. The role of systemic therapy in resectable gastric and gastro-oesophageal junction cancer. *Curr. Treat. Options Oncol.* **18**, 69 (2017).
- Riddell, I. A. Cisplatin and oxaliplatin: our current understanding of their actions. *Met. Ions Life Sci.* **18**, (2018).
- Martinez-Balibrea, E. et al. Tumor-related molecular mechanisms of oxaliplatin resistance. *Mol. Cancer Ther.* **14**, 1767–1776 (2015).
- Ren, W. W. et al. MicroRNA-125b reverses oxaliplatin resistance in hepatocellular carcinoma by negatively regulating EVA1A mediated autophagy. *Cell Death Dis.* **9**, 547 (2018).
- Liu, W. et al. HMGB1-mediated autophagy modulates sensitivity of colorectal cancer cells to oxaliplatin via MEK/ERK signaling pathway. *Cancer Biol. Ther.* **16**, 511–517 (2015).
- Walczak, M. & Martens, S. Dissecting the role of the Atg12-Atg5-Atg16 complex during autophagosome formation. *Autophagy* **9**, 424–425 (2013).
- Wible, D. J., Chao, H. P., Tang, D. G. & Bratton, S. B. ATG5 cancer mutations and alternative mRNA splicing reveal a conjugation switch that regulates ATG12-ATG5-ATG16L1 complex assembly and autophagy. *Cell Discov.* **5**, 42 (2019).
- Hong, Z. P., Wang, L. G., Wang, H. J., Ye, W. F. & Wang, X. Z. Wogonin exacerbates the cytotoxic effect of oxaliplatin by inducing nitrosative stress and autophagy in human gastric cancer cells. *Phytomedicine* **39**, 168–175 (2018).
- Jeong, S. et al. Cannabidiol overcomes oxaliplatin resistance by enhancing NOS3- and SOD2-induced autophagy in human colorectal cancer cells. *Cancers* **11**, 781 (2019).
- Czarny, P., Wigner, P., Galecki, P. & Sliwinski, T. The interplay between inflammation, oxidative stress, DNA damage, DNA repair and mitochondrial dysfunction in depression. *Prog. Neuro Psychopharmacol. Biol. Psychiatry* **80**, 309–321 (2018).
- Wang, S. et al. PRDX2 protects against oxidative stress induced by H. pylori and promotes resistance to cisplatin in gastric cancer. *Redox Biol.* **28**, 101319 (2020).
- Wei, L. et al. The emerging role of microRNAs and long noncoding RNAs in drug resistance of hepatocellular carcinoma. *Mol. Cancer* **18**, 147 (2019).
- Lee, S. et al. Noncoding RNA NORAD regulates genomic stability by sequestering PUMILIO proteins. *Cell* **164**, 69–80 (2016).
- Sun, Y. et al. LINC00657 played oncogenic roles in esophageal squamous cell carcinoma by targeting miR-615-3p and JunB. *Biomed. Pharmacother.* **108**, 316–324 (2018).
- Chen, T., Qin, S., Gu, Y., Pan, H. & Bian, D. Long non-coding RNA NORAD promotes the occurrence and development of non-small cell lung cancer by adsorbing MiR-656-3p. *Mol. Genet. Genomic Med.* **7**, e757 (2019).

21. He, H., Yang, H., Liu, D. & Pei, R. LncRNA NORAD promotes thyroid carcinoma progression through targeting miR-202-5p. *Am. J. Transl. Res.* **11**, 290–299 (2019).
22. Haeussler, M. et al. The UCSC Genome Browser database: 2019 update. *Nucleic Acids Res.* **47**, 853–858 (2019).
23. Kimura, H. Histone modifications for human epigenome analysis. *J. Hum. Genet.* **58**, 439–435 (2013).
24. Attar, N. & Kurdistani, S. K. Exploitation of EP300 and CREBBP lysine acetyltransferases by cancer. *Cold Spring Harb. Perspect. Med.* **7**, a026534 (2017).
25. Blobel, G. A. CREB-binding protein and p300: molecular integrators of hematopoietic transcription. *Blood* **95**, 745–755 (2000).
26. Armas-Lopez, L. et al. Epigenomic study identifies a novel mesenchyme homeobox2-GLI1 transcription axis involved in cancer drug resistance, overall survival and therapy prognosis in lung cancer patients. *Oncotarget* **8**, 67056–67081 (2017).
27. Li, J. H. et al. starBase v2.0: decoding miRNA-ceRNA, miRNA-ncRNA and protein-RNA interaction networks from large-scale CLIP-Seq data. *Nucleic Acids Res.* **42**, 92–97 (2014).
28. Shi, Q. et al. MiR-433-3p inhibits proliferation and invasion of esophageal squamous cell carcinoma by targeting GRB2. *Cell. Physiol. Biochem.* **46**, 2187–22196 (2018).
29. Sun, S. et al. MiR-433-3p suppresses cell growth and enhances chemosensitivity by targeting CREB in human glioma. *Oncotarget* **8**, 5057–5068 (2017).
30. Dilruba, S. & Kalayda, G. V. Platinum-based drugs: past, present and future. *Cancer Chemother. Pharmacol.* **77**, 1103–1124 (2016).
31. Wang, G. et al. Efficacy and safety of oxaliplatin-based regimen versus cisplatin-based regimen in the treatment of gastric cancer: a meta-analysis of randomized controlled trials. *Int. J. Clin. Oncol.* **24**, 614–623 (2019).
32. Fritsch, R. & Hoepfner, J. Oxaliplatin in perioperative chemotherapy for gastric and gastroesophageal junction (GEJ) adenocarcinoma. *Expert Rev. Gastroenterol. Hepatol.* **13**, 285–291 (2019).
33. Kanaji, S. et al. Recent updates in perioperative chemotherapy and recurrence pattern of gastric cancer. *Ann. Gastroenterol. Surg.* **2**, 400–405 (2018).
34. Zhu, Q. et al. Regulation of OCT2 transcriptional repression by histone acetylation in renal cell carcinoma. *Epigenetics* **14**, 791–803 (2019).
35. Luo, Y. J. et al. Non-coding RNA in drug resistance of gastric cancer. *World J. Gastrointest. Oncol.* **11**, 957–970 (2019).
36. YiRen, H. et al. Long noncoding RNA MALAT1 regulates autophagy associated chemoresistance via miR-23b-3p sequestration in gastric cancer. *Mol. Cancer* **16**, 174 (2017).
37. Dong, H. et al. Activation of LncRNA TINCR by H3K27 acetylation promotes Trastuzumab resistance and epithelial-mesenchymal transition by targeting MicroRNA-125b in breast Cancer. *Mol. Cancer* **18**, 3 (2019).